NANO LETTERS

2004
Vol. 4, No. 12
2367−2371

Polyol Synthesis of Platinum Nanoparticles: Control of Morphology with Sodium Nitrate

Thurston Herricks,[†] Jingyi Chen,[‡] and Younan Xia*[,‡]

Department of Materials Science and Engineering and Department of Chemistry, University of Washington, Seattle, Washington 98195

Received September 1, 2004; Revised Manuscript Received October 25, 2004

ABSTRACT

Morphological control over platinum nanoparticles was realized by varying the amount of $NaNO_3$ added to a polyol process, where H_2PtCl_6 was reduced by ethylene glycol to form $PtCl_4^{2-}$ and Pt^0 at 160 °C. As the molar ratio between $NaNO_3$ and H_2PtCl_6 was increased from 0 to 11, the morphology of Pt nanoparticles evolved from irregular spheroids with rounded profiles to tetrahedra and octahedra with well-defined facets. Absorption spectroscopy studies suggest that nitrate was reduced to nitrite by $PtCl_4^{2-}$ in the early stage of the synthesis, and the nitrite could then form stable complexes with both Pt(II) and Pt(IV) species. As a result, the reduction of Pt precursors by ethylene glycol was greatly slowed. This change in reaction kinetics altered the growth rates associated with different crystallographic directions of the Pt nanocrystals and ultimately led to the formation of different morphologies.

Introduction. A great deal of effort has been directed toward the synthesis of nanoparticles having well-controlled shapes. In addition to size, the shape of a nanocrystal may provide another useful parameter to control when one needs to tailor the electronic, optical, magnetic, or chemical properties of a solid material. Synthetic work on II−IV semiconductors, metals, and metal oxides has yielded monodisperse colloidal samples in the form of spheres, thin plates, rods, wires, polyhedrons (cube, tetrahedron, and octahedron), and tetrapods.[1] In addition to their use in many fundamental studies, these faceted nanoparticles are being extensively pursued for use as active components in the fabrication of electronic, photonic, and information storage devices through the self-assembly approach.

Use of organic surfactants and polymers in nanoparticle synthesis has been a popular method of achieving morphological control. Investigation is just beginning on the role(s) of inorganic species in controlling the shape. To this end, Murphy et al. have demonstrated the synthesis of silver nanowires by controlling the amount of NaOH added to the reaction solution, without the use of any polymer or surfactant.[2] Pileni et al. have shown that addition of some inorganic salts could control the shape of copper nanoparticles in a $Cu(AOT)_2$−isooctane−water system when the micelle template in this system was kept the same.[3] Our group has also established that silver nanocubes with truncated corners can be reproducibly synthesized in large quantities by adding a trace amount of NaCl to the reaction solution of a polyol synthesis.[4] The chloride ions are thought to have effects on the stability and solubility of small crystallites that serve as seeds in the subsequent growth step. Furthermore, we have discovered that a trace amount of iron species (Fe^{2+} or Fe^{3+}) in the reaction mixture could significantly alter the growth kinetics of different crystallographic directions of platinum and thus induce an anisotropic growth mode resulting in the formation of uniform nanowires with relatively high aspect ratios.[5] These examples clearly demonstrate that introduction of inorganic species may provide a means as powerful as organic surfactants and polymers for controlling the shape of metallic nanoparticles. For the polyol synthesis, inorganic ions are expected to have a more pronounced influence on the nucleation of nanocrystallites than organic surfactants or polymers because of their relatively smaller sizes and increased ability to form complexes with reactive species in the solution. Here we report a case study where the reduction kinetics and thus morphology of Pt nanoparticles could be controlled through the use of inorganic species such as sodium nitrate.

Platinum nanoparticles have been extensively studied for their unique catalytic properties.[6] The catalytic performance of Pt nanoparticles is also highly dependent on the exact arrangement between atoms on the exposed facets.[7] Production of monodisperse, uniformly faceted particles is desired for high specificity in a catalytic process. Platinum nanoparticles can be synthesized using a number of different methods.[8] In general, the synthesis involves the reduction

* Corresponding author. E-mail: xia@chem.washington.edu.
[†] Department of Materials Science and Engineering.
[‡] Department of Chemistry.

10.1021/nl048570a CCC: $27.50
Published on Web 11/17/2004

of a Pt(II) or Pt(IV) precursor in the presence of a stabilizing polymer by reducing agents such as alcohols, sodium borohydride, or hydrogen gas. While the resultant nanoparticles may be considered monodisperse in size, they are often irregular in shape or lack well-defined facets. Generating faceted colloids has been demonstrated using a sodium borohydride reduction in water at 0 °C, followed by phase transfer to an organic solvent.[8e] Another chemical method of generating faceted platinum particles involves the use of hydrogen as a reducing agent in water and sodium polyacrylate as a capping agent.[8f] The mechanism responsible for the formation of faceted particles is yet to be elucidated. For the system described in this work, it is believed that the morphological evolution is controlled by the reduction kinetics of the Pt (IV) precursor.

Experimental Section. In a typical synthesis, 1 mL of 80 mM H_2PtCl_6 solution in ethylene glycol was rapidly added to 7 mL ethylene glycol (held at 160 °C) that contained both $NaNO_3$ and poly(vinyl pyrrolidone) (PVP, MW = 55 000, Aldrich, 30 mM as calculated in terms of the repeating unit). The concentration of H_2PtCl_6 was fixed at 10 mM for all syntheses, while the concentration of $NaNO_3$ was varied in the range from 0 to 110 mM. In this so-called polyol synthesis,[11] ethylene glycol serves as both solvent and reducing agent. For spectroscopic measurements, a 0.3 mL aliquot of the sample was removed from the reaction solution every 30 s using a 19-gauge stainless steel needle and cooled in air to room temperature. Brief insertion of the metallic needle into the reaction mixture did not significantly alter the final product as confirmed by TEM, nor did it change the observed rate of color change. 30 μL of this sampled solution was then diluted with 3 mL of ethanol for UV−vis spectral measurements with a HP 8452A diode array spectrophotometer. Samples for TEM studies were precipitated with acetone and then suspended in ethanol using brief sonication. A small drop of the particle suspension was placed on a Formvar grid (Ted Pella) and allowed to evaporate slowly under ambient conditions. The TEM images were taken on a Phillips EM420T or a Tecnai G_2 F20.

Results and Discussion. We followed the morphological evolution of Pt nanoparticles using TEM. Figure 1 shows typical TEM images of Pt nanoparticles that were obtained when different amounts of $NaNO_3$ were added to the synthetic solutions. These images clearly indicate a change in morphology as the concentration of $NaNO_3$ was gradually increased. Particles synthesized without the presence of $NaNO_3$ were irregular in shape and their sizes varied on the scale of 3−5 nm (Figure 1a). At the highest concentration (Figure 1f), both octapod and tetrapod particles with dimensions >30 nm were found with relatively high yields in the final product. When the concentration of $NaNO_3$ was controlled between these two extremes (Figure 1, b−d), the products exhibited a transition from irregular particles (Figure 1b), through a sample with bimodal size distribution (Figure 1c), to uniform colloids (Figure 1d). In general, presence of $NaNO_3$ at sufficiently high concentrations (Figure 1, d and e) would cause the particles to take on shapes with the kind of symmetry expected for a face-center-cubic (fcc) metal.

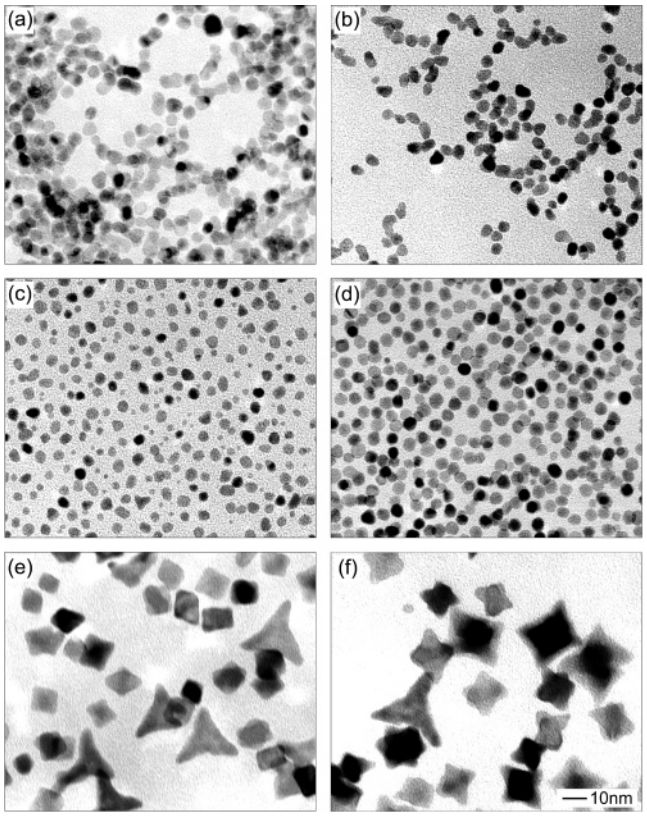

Figure 1. TEM images of Pt nanoparticles synthesized with different ratios between $NaNO_3$ and H_2PtCl_6: (a) 0, (b) 0.3, (c) 1.6, (d) 3.3, (e) 5.5, and (f) 11.0. It is clear that the exact ratio between $NaNO_3$ and H_2PtCl_6 had a profound influence on the morphology of resultant nanoparticles. The 10-nm scale bar is applicable to all images.

An increase in the concentration of $NaNO_3$ also altered the size uniformity and average diameter of the resultant Pt nanoparticles. Note that PVP had to be present in all these syntheses. Otherwise, the Pt nanoparticles would agglomerate into irregular, large structures. Since all syntheses shown in Figure 1 contained the same amount of PVP in their solutions, these results clearly indicate that it was $NaNO_3$ rather than PVP that caused the formation of different morphologies.

Figure 2 shows high resolution TEM images taken from individual Pt particles, illustrating the subtle change in morphology when the ratio between $NaNO_3$ and H_2PtCl_6 was changed from 5.5 (Figure 2, a and e) to 11.0 (Figure 2, b and f). A model of the particle is shown in the drawing below each TEM image. In Figure 2a, an octahedral particle is displayed in the [110] orientation, as verified by the fast Fourier transform pattern of this image. The corners of this octahedron point toward the ⟨100⟩ directions. This octahedral crystal is hence bounded by {111} facets (Figure 2c). An increase in the concentration of $NaNO_3$ caused additional changes to the particle morphology. As shown in Figure 2b, the particle is also oriented along the [110] axis with the corners pointing toward the ⟨100⟩ directions. However, continued growth is noticed at the octahedron's corners as they bulge beyond facets in the ⟨100⟩ directions. For the

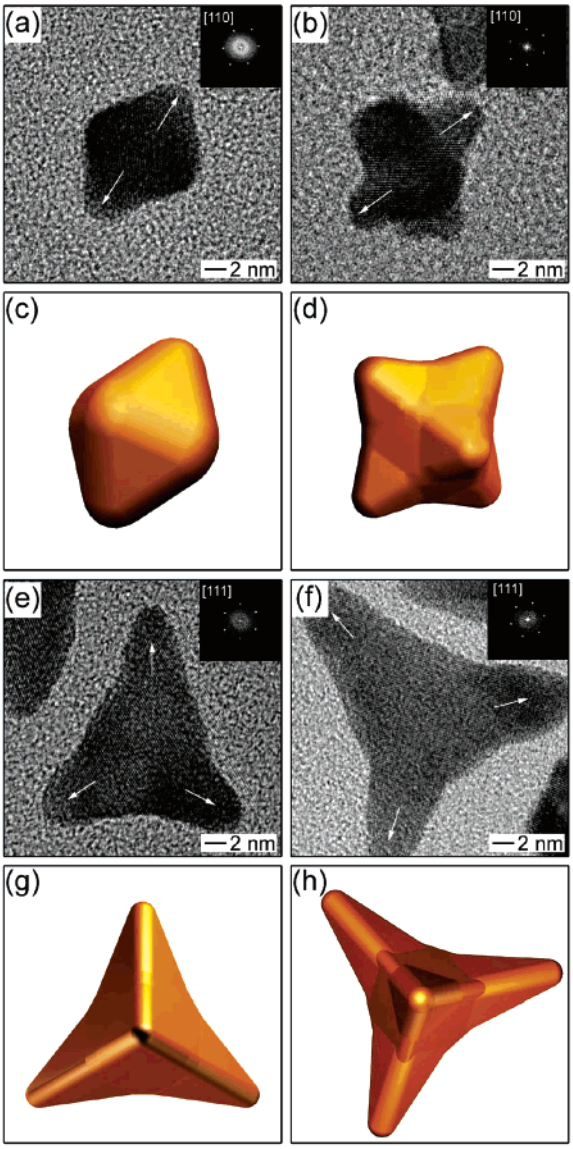

Figure 2. HRTEM images of Pt nanoparticles that were obtained with the molar ratio between $NaNO_3$ and H_2PtCl_6 being controlled at (a, e) 5.5 and (b, f) 11.0, respectively. The insets show fast Fourier transform (FFT) patterns used to determine the crystallographic directions marked in the insets. (c, d, g, h) Models showing that the growth of Pt nanoparticle (see the HRTEM image immediately above each drawing) was substantially enhanced at ridges and corners to form both octapods and tetrapods.

particle shown in Figure 2a, no significant growth in the ⟨111⟩ directions is detected.

The same trend was also observed for the tetrahedral nanoparticles where growth occurred at particle corners and edges. As shown in Figure 2e, the corners of the tetrahedron point toward the ⟨111⟩ directions. Figure 2f shows a tetrahedral particle synthesized at a much higher concentration of $NaNO_3$, clearly showing enhanced growth in the ⟨111⟩ directions as the arms of this particle become more prominent to appear like a tetrapod. This is in contrast to the octahedral particle depicted in Figures 2a and 2b, where growth was mainly observed along the ⟨100⟩ directions. These observations show that growth of an individual Pt particle is predominant in either ⟨111⟩ directions or ⟨100⟩ directions. In the present system, the nanoparticles experienced higher growth rates at areas of high curvature; specifically, the corners and edges. Slower growth rates were observed at the centers of facets.

Chernov and others have observed and modeled this type of growth as the basis for growth in dendrite systems.[10] Specifically, they investigate how the morphology of a particle evolves under two different conditions. The first condition is when the diffusion of an adatom is very fast compared to the rate an add-atom is adsorbed onto the growing particle surface. In this case, the level of supersaturation is identical in regions very close to the particle's surface and far away from the particle. Any ridge that forms on the surface has a supersaturation level virtually identical to any other location on the growing crystal and is therefore not favored. The crystal will then grow into a shape that is dominated by the surface kinetics. Therefore, the crystal does not change its shape significantly over time. From particle morphologies observed in Figures 1a−1d, this appears to be the situation when Pt particles are synthesized when $NaNO_3$ is not present or at relatively low concentrations of $NaNO_3$.

The second condition Chernov described was where diffusion of an add-atom from solution to a growing crystal surface is slow compared to the rate a growth unit is adsorbed onto the particle surface. In this situation, a gradient occurs as the supersaturation at the particle surface is low and increases with distance from the particle. If a ridge forms on the particle's surface, it will have a slightly higher supersaturation at the top of the ridge than at the base. Then growth on the ridge will be encouraged by the supersaturation gradient. With a spherical particle under these conditions, any perturbation of the particle's surface will cause the particle's edges and corners to preferentially grow. Ridge growth should occur in directions directed by the particle's surface energies and may include curvature, step density, and crystalline anisotropy.[10b] From the particle morphologies observed in Figures 1d and 1e, this second situation appears to be when Pt particles are synthesized in the presence $NaNO_3$ at relatively high concentrations.

This kinetic description can be applied to crystallization from both melt and solution systems where a supersaturation gradient occurs. In general, a supersaturation gradient does not easily form in a well-stirred solution. In the present system, however, Pt^0 must be generated through a chemical reaction. If the rate at which Pt^0 is generated in the solution is substantially reduced without altering surface properties of the particles, then a supersaturation gradient needed for anisotropic growth is expected to occur even when the solution is well stirred.

We suggest that the function of $NaNO_3$ and air is to change the reaction pathway for Pt(IV) reduction, thereby enhancing anisotropic growth of Pt nanoparticles. It is known that Pt forms complexes such as $Pt(NO_2)_6^{2-}$ with nitrite ions.[11] As a result, $PtCl_6^{2-}$ may undergo complete substitution of chlorine to form a nitroplatinate salt. In fact, the most dramatic change in particle morphology occurred when the ratio between NO_3^- and $PtCl_6^{2-}$ approached six. As indicated

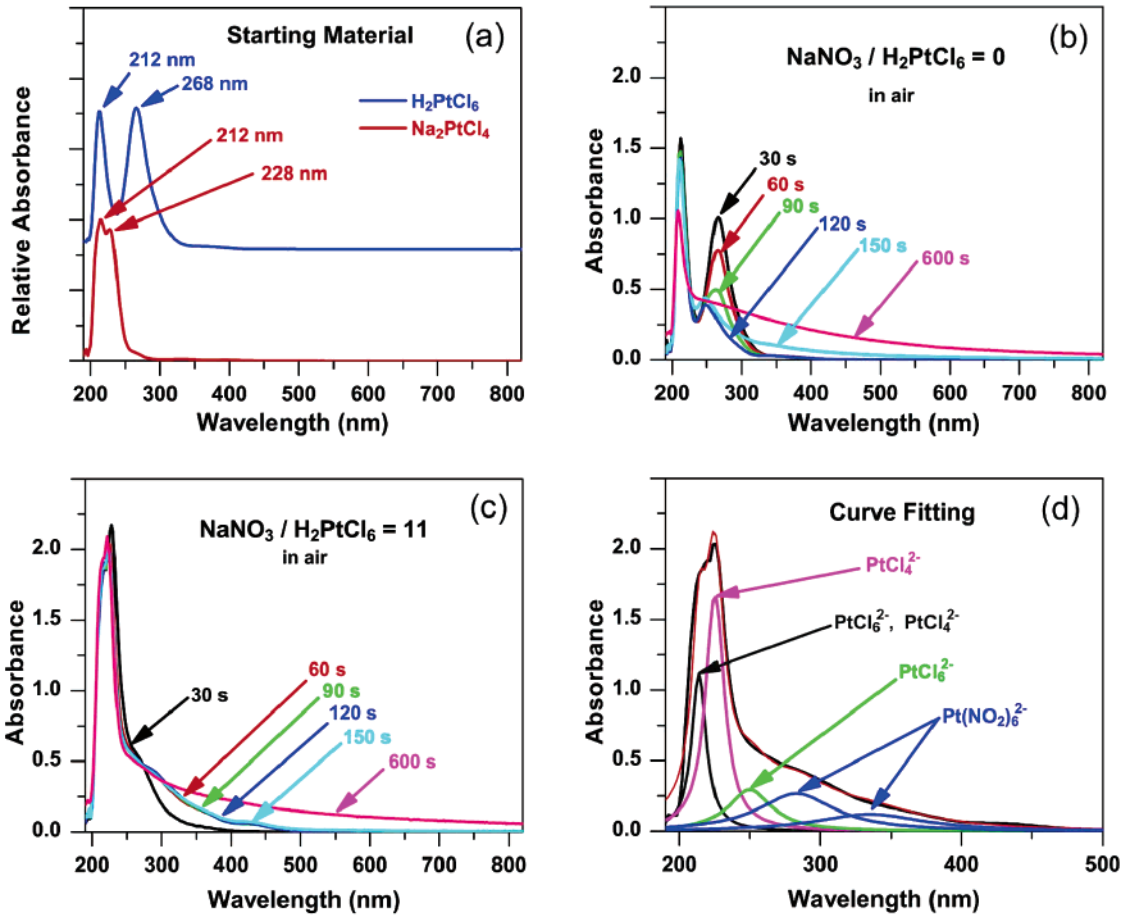

Figure 3. (a) UV−vis spectra of H_2PtCl_6 and Na_2PtCl_4 compounds taken from their stock solutions in ethylene glycol. Note that H_2PtCl_6 displays two extinction peaks located at 212 and 268 nm; and Na_2PtCl_4 shows two peaks located at 212 and 228 nm. (b, c) UV−vis spectra taken from reaction solutions at different stages of the synthesis, which was performed in ethylene glycol (b) without adding $NaNO_3$, and (c) with the addition of $NaNO_3$. (d) Curve fitting of the spectrum at $t = 60$ s indicating the formation of $Pt(NO_2)_6^{2-}$ species in the solution. This complex has distinctive peaks at 280 and 330 nm, respectively.

by previous studies, nitroplatinate complexes exhibited a much slower reduction rate as compared with the chloroplatinate salt.[12] The net result is to slow the reaction kinetics, thereby altering the final shape exhibited by the Pt nanocrystals.

These arguments are consistent with the UV−vis spectra taken at different times during the reaction (Figures 3a−c). As shown in Figure 3a, both $PtCl_4^{2-}$ and $PtCl_6^{2-}$ share absorbance peaks at 212 nm. However, $PtCl_4^{2-}$ has a strong peak at 228 nm and $PtCl_6^{2-}$ has a strong peak at 268 nm. As we recently found, reduction of Pt(IV) to Pt^0 by ethylene glycol occurs through a Pt(II) intermediate.[5] For a reaction run without $NaNO_3$, both peaks at 212 and 268 nm disappeared within 5 min as the reaction proceeded (Figure 3b). When $NaNO_3$ was added at a ratio of 11:1 for NO_3^- and $PtCl_6^{2-}$, the peak at 268 nm disappears very quickly (within 30 s) indicating rapid loss of $PtCl_6^{2-}$ (Figure 3c). We suggest that nitrite ions are formed in situ through the reduction of nitrate ions by $PtCl_4^{2-}$:

$$NO_3^- + 2H^+ + 2e^- \rightarrow NO_2^- + H_2O \quad E^\circ = 0.94 \text{ eV}$$

$$PtCl_4^{2-} + 2Cl^- \rightarrow PtCl_6^{2-} + 2e^- \quad E^\circ = -0.74 \text{ eV}$$

It is worth noting that a coupling between the above reactions could reduce the formation rate for Pt^0 in solution by pushing Pt(II) species back to the higher Pt(IV) oxidation state. Through this reaction pathway, nitrite ions may form and then ligand exchange with $PtCl_6^{2-}$ to form complexes such as $Pt(NO_2)_6^{2-}$. This complex has been reported to have strong absorption peaks at 280 and 330 nm, respectively.[13] For the present system, absorbance in the range from 250 to 350 nm is indicative of the $Pt(NO_2)_6^{2-}$ species after fitting the observed spectrum with multiple Lorentzian peaks (Figure 3d).

Our UV−vis spectroscopic studies also indicate that the reaction was sensitive to air. In the presence of air and high nitrate concentrations, a steady state where the UV−vis spectra appeared identical was observed between 60 and 150 s (Figure 3c). Such a steady state was not observed when the same synthesis was performed under argon protection. Reactions were found to reach completion when the spectral component from particle scattering no longer increased. According to the UV−vis spectra, the reaction under air did not reach completion until $t = 600$ s, whereas the argon-protected reaction was completed at $t = 90$ s. Figure 4 shows TEM images of Pt nanoparticles synthesized under the

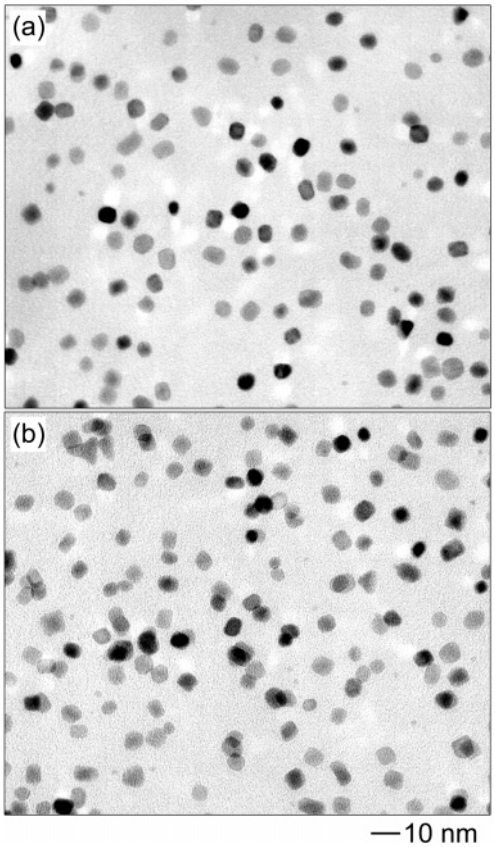

Figure 4. TEM images of as-obtained Pt nanoparticles when the polyol synthesis was conducted under (a) argon and (b) nitrogen protection. The molar ratio between $NaNO_3$ and H_2PtCl_6 was maintained at 11.

protection of argon and nitrogen gas. The nanoparticles grown under argon protection have a cubic morphology (Figure 4a) and sizes on the order of 7−10 nm. These results are identical to those observed when particles were synthesized under nitrogen (Figure 4b). The observed difference in morphology between particles grown in air (Figure 1f) and particles grown under inert atmosphere (Figure 4) correlates with theory stated earlier that slower reduction kinetics will lead to particles with a more anisotropic morphology. At the current stage of development, it is still not clear about the exact role(s) played by air in this synthesis. Because Pt nanoparticles synthesized under nitrogen were morphologically similar to those obtained under argon, we believed that the morphological difference observed between the products shown in Figure 4 and Figure 1f was mainly caused by components (e.g., oxygen and/or water vapor) other than nitrogen contained in a typical sample of air.

Conclusion. We have shown that addition of sodium nitrate to a polyol process could alter the morphology of Pt nanoparticles. The key to the success of this morphological control was nitrate anion, whose function was to substantially slow the reduction of Pt(II) and Pt(IV) species by ethylene glycol. We suggest that this mediation could be ascribed to the formation of stable complexes between the Pt(II) and Pt(IV) species and nitrite ions in solution and thereby alter the reaction kinetics. Although PVP has been found to play an important role in controlling the morphology of silver[1d] and gold[1k] nanostructures, it is believed that PVP does not provide such a control for Pt nanostructures other than stabilizing them through the steric effect. This is probably related to their difference in surface chemistry as well as physical dimensions (~10 nm for Pt nanostructures vs >50 nm for Ag and Au nanostructures). Further investigations will enable us to elucidate the reaction mechanism and lead to a precise control over the morphology of Pt nanostructures.

Acknowledgment. This work has been supported in part by a DAPRA-DURINT subcontract from Harvard University and a Science and Engineering Fellowship from the David and Lucile Packard Foundation. T.H. and J.C. are partially supported by an IGERT (funded by NSF, DGE−9987620) and a UIF fellowship from the Center for Nanotechnology at the UW, respectively. Work was performed in part at the University of Washington Nanotech User Facility (NTUF), a member of the National Nanotechnology Infrastructure Network (NNIN), which is supported by the National Science Foundation. T.H. thanks Professors Y. K. Rao and Lucien Brush for their valuable suggestions regarding this project, and David Joswiak and Professor Don Brownlee for the use of their TEM.

References

(1) See, for example, (a) Wang, Z. L. *J. Phys. Chem. B.* **2000**, *104*, 1153. (b) Sun, S.; Murray, C. B.; Weller, D.; Folks, L.; Moser, A. *Science* **2000**, *287*, 1989. (c) Puntes, V. P.; Krishnan, K.; Alivisatos, A. P. *Science* **2001**, *291*, 2115. (d) Sun, Y.; Xia, Y. *Science* **2002**, *298*, 2176. (e) Xia, Y.; Yang, P.; Sun, Y.; Wu, Y.; Mayers, B.; Gates, B.; Yin, Y.; Kim, F.; Yan, H. *Adv. Mater.* **2003**, *15*, 353. (f) Teng, X.; Yang, H. *J. Am. Chem. Soc.* **2003**, *125*, 14559. (g) Chen, S.; Wang, Z. L.; Ballato, J.; Foulger, S.; Carroll, D. *J. Am. Chem. Soc.* **2003**, *125*, 16186. (h) Peng, X. *Adv. Mater.* **2003** *15*, 459. (i) Joo, J.; Na, H.; Yu, T.; Kim, Y.; Wu, F.; Zhang, J.; Hyeon, T. *J. Am. Chem. Soc.* **2003**, *125*, 11100. (j) Sau, T. K.; Murphy, C. J. *J. Am. Chem. Soc.* **2004**, *126*, 8648. (k) Kim, F.; Connor, S.; Song, H.; Kuykendall, T.; Yang, P. *Angew. Chem., Int. Ed.* **2004**, *43*, 3673.

(2) Caswel, K. K.; Bender, C. M.; Murphy, C. J. *Nano Lett.* **2003**, *4*, 667.

(3) Pileni, M. P. *Nature Mater.* **2003**, *2*, 145.

(4) Wiley, B.; Herricks, T.; Sun, Y.; Xia, Y. *Nano Lett.* **2004**, *4*, 1733.

(5) Chen, J.; Herricks, T.; Geissler, M.; Xia, Y. *J. Am. Chem. Soc.* **2004**, *126*, 10854.

(6) See, for example, Narayanan, R.; El-Sayed, M. A. *J. Phys. Chem. B* **2003**, *107*, 12416.

(7) (a) Falicov, L. M.; Somorjai, G. A. *Proc. Natl. Acad. Sci. U.S.A.* **1985**, *82*, 2207. (b) Narayanan, R.; El-Sayed, M. A. *Nano Lett.* **2004**, *4*, 1343.

(8) See, for example, (a) Teraanishi, T.; Hosoe, M.; Tanaka, T.; Miyake, M. *J. Phys. Chem. B* **1999**, *103*, 3818. (b) Chen, C.; Akashi, M. *Langmuir* **1997**, *13*, 6465. (c) Duff, D.; Edwards, P.; Johnson, B. *J. Phys. Chem.* **1995**, *99*, 15934. (d) Yang, J.; Lee, J.; Deivaraj, T.; Too, H. *Langmuir* **2003**, *19*, 10361. (e) Zhao, S.; Chen, S.; Wang, S.; Lie, D.; Ma, H. *Langmuir* **2002**, *18*, 3315. (f) Ahmadi, T.; Wang, Z.; Green, T.; Henglein, A.; El-Sayd, M. *Science* **1996**, *272*, 1924.

(9) Feivet, F.; Lagier, J. P.; Figlarz, M. *MRS Bull.* **1989**, *December*, 29.

(10) (a) Nielsen, A. *Kinetics of Precipitation*; Pergamon Press Ltd.: New York, 1964. (b) Chernov, A. *Sov. Phys.-Crystallogr.* **1972**, *16*, 734.

(11) Blinov, I.; Balashev, K.; Shagisultanova, G. *Koord. Khim.* **1986**, *11*, 644.

(12) Turkevich, J.; Miner, R. S., Jr. *J. Phys. Chem.* **1986**, *90*, 4765.

(13) Shubochkin, L.; Shubochkina, E.; Lapin, V.; Kharitonov Y. *Koord. Khim.* **1978**, *4*, 581.

NL048570A